



Retention modeling for ultra-thin density of Cu-based conductive bridge random access memory (CBRAM)

Cite as: AIP Advances 6, 025203 (2016); <https://doi.org/10.1063/1.4941752>

Submitted: 23 December 2015 . Accepted: 27 January 2016 . Published Online: 05 February 2016

Fekadu Gochole Aga , Jiyong Woo, Sangheon Lee, Jeonghwan Song, Jaesung Park , Jaehyuk Park, Seokjae Lim, Changhyuck Sung, and Hyunsang Hwang



View Online



Export Citation



CrossMark

ARTICLES YOU MAY BE INTERESTED IN

[Enhancement of resistive switching properties in nitride based CBRAM device by inserting an Al₂O₃ thin layer](#)

Applied Physics Letters **110**, 203102 (2017); <https://doi.org/10.1063/1.4983465>

[A numerical study of multi filament formation in metal-ion based CBRAM](#)

AIP Advances **6**, 025212 (2016); <https://doi.org/10.1063/1.4942209>

[Field-induced nucleation in threshold switching characteristics of electrochemical metallization devices](#)

Applied Physics Letters **111**, 063109 (2017); <https://doi.org/10.1063/1.4985165>

AVS Quantum Science

Co-published with AIP Publishing



Coming Soon!

Retention modeling for ultra-thin density of Cu-based conductive bridge random access memory (CBRAM)

Fekadu Gochole Aga, Jiyong Woo, Sangheon Lee, Jeonghwan Song, Jaesung Park, Jaehyuk Park, Seokjae Lim, Changhyuck Sung, and Hyunsang Hwang^a

Department of Material Science and Engineering, Pohang University of Science and Technology(POSTECH), 77 Cheongam-ro, Nam-gu, Pohang 790-784, South Korea

(Received 23 December 2015; accepted 27 January 2016; published online 5 February 2016)

We investigate the effect of Cu concentration On-state resistance retention characteristics of W/Cu/Ti/HfO₂/Pt memory cell. The development of RRAM device for application depends on the understanding of the failure mechanism and the key parameters for device optimization. In this study, we develop analytical expression for cations (Cu⁺) diffusion model using Gaussian distribution for detailed analysis of data retention time at high temperature. It is found that the improvement of data retention time depends not only on the conductive filament (CF) size but also on Cu atoms concentration density in the CF. Based on the simulation result, better data retention time is observed for electron wave function associated with Cu⁺ overlap and an extended state formation. This can be verified by analytical calculation of Cu atom defects inside the filament, based on Cu⁺ diffusion model. The importance of Cu diffusion for the device reliability and the corresponding local temperature of the filament were analyzed by COMSOL Multiphysics simulation. © 2016 Author(s). All article content, except where otherwise noted, is licensed under a Creative Commons Attribution (CC BY) license (<http://creativecommons.org/licenses/by/4.0/>). [<http://dx.doi.org/10.1063/1.4941752>]

A variety of resistive switching memory technologies are currently under investigation. The intention is to develop new memory devices that are able to compete or even to replace existing conventional technologies. Among these emerging technologies, conductive bridge random access memory (CBRAM) has been extensively studied for applications in next generation nonvolatile memory due to its characteristics of low power consumption, high speed operation, ease of fabrication and high density integration.¹⁻⁴ The switching of CBRAM is generally attributed to the formation and rupture of metallic conductive filament (CF) due to the migrations of the active metal ions (Ag⁺ and Cu⁺) in solid electrolyte.⁵⁻⁷ We use the HfO₂ as solid electrolyte due to the significant interest in the application of optimal high-k gate dielectric in advance metal oxide semiconductor (MOS) devices, which offers the ease of integration with CMOS process compatibility. Furthermore, HfO₂ has several merits of thermodynamic stability.⁸

In CBRAM the reliability challenges are still open and have to be investigated in detail. For practical application, the CBRAM retention property is of utmost importance. The retention characteristics have already been reported for switching memory cells utilizing different materials for the oxide layers and electrodes.^{9,10} In particular size dependent reliability model of RRAM based on metallic filament conduction is introduced.¹¹ However; retention characteristics using analytical model in terms of cations concentration has up to now remained elusive. In this study, we address the impact of cations concentration on the retention property of On-state resistance rather than size of filament and analyzed the retention time under different temperature for various resistance of low resistance state (R_{LRS}). The retention time is improved for electron wave function associated with overlapped Cu⁺ and extended state formation.¹² Conduction in the set state is described in our

^aE-mail address of corresponding author: hwanghs@postech.ac.kr

model by transport in a localized region with high concentration of defects. We assume that the R_{LRS} is controlled by concentration rather than filament size. The filament is composed of Cu atoms regularly distributed in the resistive layer.

We fabricate Ti/HfO₂/Pt and W/Cu/Ti/HfO₂/Pt devices having 250nm via-hole in Pt/Ti/SiO₂/Si substrate with Pt bottom electrode (BE). At first Pt (~50nm) as BE was deposited on Ti/SiO₂/Si substrate by dc sputtering. Next 100nm SiO₂ layer was deposited by PECVD followed patterning and etching of 250nm via-hole by conventional lithography and reactive ion etching systems. A high-K HfO₂ solid electrolyte with a thickness of 4nm was deposited by atomic layer deposition. For the first device, Ti used as top electrode (TE) with thickness 3nm was deposited by dc sputtering with Ar flow rate of 30 sccm and dc power of 100W. For second device, Cu which provided mobile ions was deposited at a layer thickness of 30nm by dc sputtering on 3nm Ti buffer layer. Finally, 50nm thick layer of tungsten (W) was then deposited by dc sputtering to protect the Cu surface layer from oxidation by the external environment. The total thickness of the top electrode (W + Cu) was approximately 80nm for Cu TE based device. The dc power for Cu and W deposition was 100W and working pressure was 5mTorr. The device schematic is shown in Fig. 1(a) for Cu TE based device. The bias applied to TE and the BE was grounded during I-V measurements for both devices. Fig. 1(b) shows the quasi-static Cu-based CBRAM (W/Cu/HfO₂/Pt) bipolar characteristic. The device with Ti TE (Ti/HfO₂/Pt) without Cu top shows small OFF/ON ratio as depicted in Fig. 1(c). The device with Cu TE using Ti as buffer layer show stable resistance switching and superior data retention with resistance ratio greater than 10⁴.

The On-state resistance of the CBRAM device is controlled by defect concentration (Cu atoms) in the filament. When the defect concentration in the filament increase, the On-state resistance decrease as shown in Fig. 2(a) and its local conductivity increase according to the empirical behavior as depicted in Fig. 2(b). Resistance degradation (retention characteristic) should be a

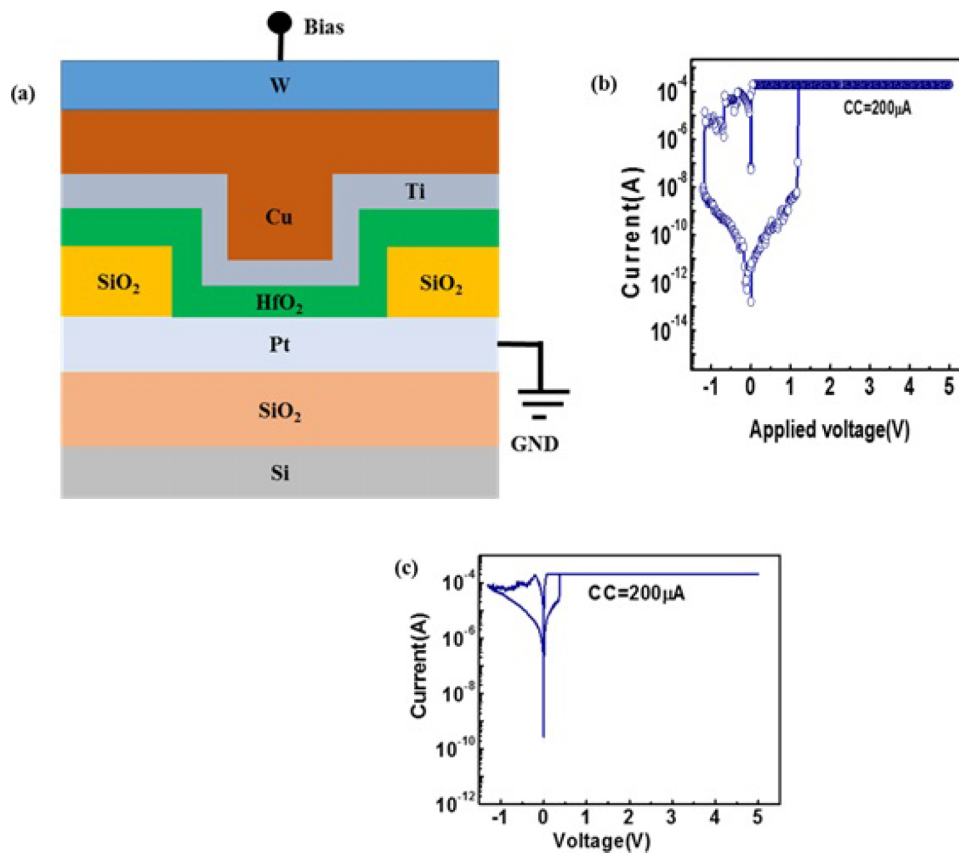


FIG. 1. (a) Schematic of Cu-based device fabrication. (b) Typical I-V characteristic of the Cu-based device. (c) I-V characteristic of Ti TE device.

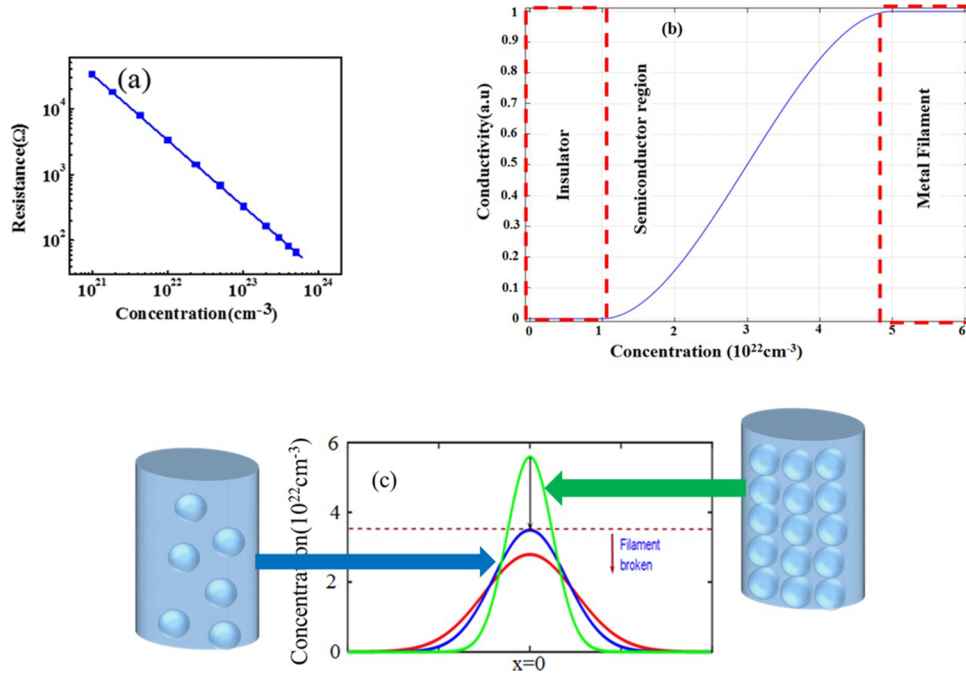


FIG. 2. (a) On-state resistance versus Cu concentration. (b) Calculated conductivity as function of Cu concentration in the filament. (c) Cu concentration profile predicted from simple analytical model using Gaussian law and its critical concentration density at $3.5 \times 10^{22} \text{ cm}^{-3}$.

function of the Cu concentration in solid electrolyte. In this model, we analyze the retention time of On-state resistance controlled by Cu concentration in the filament for different temperature.

Retention failure is described in terms of the dissolution of a conductive filament, which is enhanced by thermal activated diffusion of defects.^{13–15} Cu atoms concentration diffuse out in the hottest region due to current density along the CF, resulting in a drop of concentration density in the filament. This makes Cu concentration density decreases below the critical value and the electron wave functions associated with Cu⁺ no longer overlap and an extended state is no longer formed. Thus, the filament is effectively ruptured and the conductivity undergoes an abrupt reduction. This can be interpreted by oxidation process of Cu metallic filament and analytically calculated the Cu atoms defects inside the filament based on cations diffusion model. For our analytical modeling expression, the Cu concentration in the filament is adjusted in the x-axis in order to take into account the cylindrical shape of the filament and considering Cu concentration is higher in the center of the filament than close to the edges. The Cu concentration profile was predicted by Gaussian description using the simple analytical model of Eq. (1) [Fig. 2(c)]. The Gaussian description of Cu concentration diffusion is given by

$$C_{Cu}(x,t) = \frac{C_0}{\sqrt{\pi Dt}} \exp\left(-\frac{X^2}{4Dt}\right) \quad (1)$$

C_0 is the total number of Cu ions concentration over the device area, C_{Cu} is Cu concentration at position x away from center of filament at time t and temperature T and D is the diffusion coefficient determined by the temperature and given in the form of $D = D_0 \exp(-E_{AC}/kT)$, (D_0 is pre-exponential diffusion coefficient ($39 \text{ cm}^2/\text{s}$) and E_{AC} is activation energy for Cu⁺ diffusion ($E_{AC} = 3.4 \text{ eV}$).¹⁶

The retention failure is occurred when Cu peak concentration ($x=0$) becomes smaller than the critical Cu density. The detailed analysis of data retention time at high temperature is describe by developing the Cu atom diffusion model and we adapted conduction model from,¹⁷ where the conductivity depends on defects density (Cu concentration).

$$\sigma = \gamma C_{Cu} \exp\left(-\frac{E_A}{kT}\right) \quad (2)$$

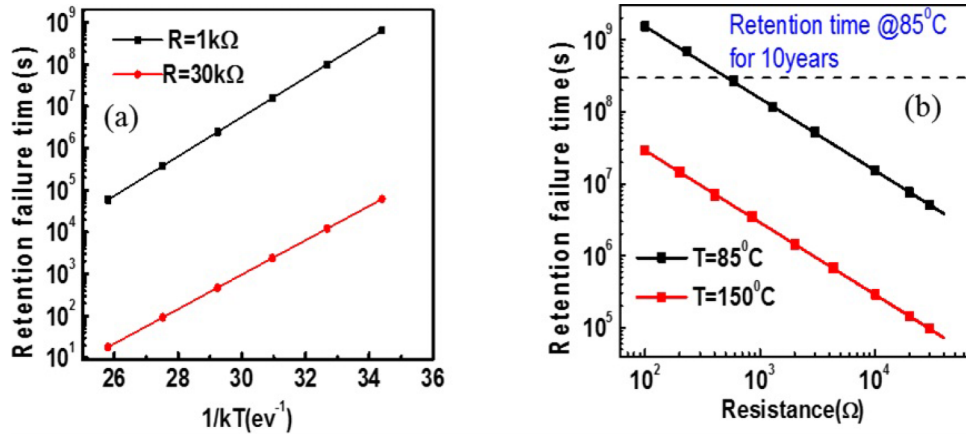


FIG. 3. (a) Dependence of retention failure time on temperature. (b) Retention failure time of On-state resistance for 85°C and 150°C temperature. 10 years expected retention time at 85°C based on extrapolated.

Where σ is conductivity, E_A is activation energy for conduction, γ is pre-factor and its value for this simulation is 10^{-20}Sm^{-1} , k =Boltzmann constant, T is absolute temperature. The E_A estimated from the slope of line fitting in Fig. 3(a) is about 0.4eV. Substituting the Gaussian diffusion Eq. (1) into the conductivity of Eq. (2), we obtained conductivity as function of Cu atom diffusion time.

$$\sigma = \gamma \exp\left(-\frac{E_A}{kT}\right) \left[\frac{C_0}{\sqrt{\pi Dt}} \exp\left(-\frac{X^2}{4Dt}\right) \right] \quad (3)$$

At high temperature the filament is more sensible to the Cu out-diffusion, leading to LRS instability by decreasing Cu defect concentration, as depicted in Fig. 3(a) and this is the main reason for retention failure. This instability of LRS due to concentration drift requires to be investigated to improve device reliability and performance. Fig. 3(b) shows the retention failure time at temperature of 85°C and 150°C for various on-state resistance. Joule heating due to current density in the filament accelerates the isotropic diffusion of Cu concentration. The diffusion of Cu metal ions out of the CF causes a decrease of Cu atoms concentration in the CF, resulting in the degradation of R_{LRS} . We obtained the On-state resistance as function of Cu concentration:

$$R_{LRS} = \frac{L}{A\gamma \frac{C_0}{\sqrt{\pi Dt}} \exp\left(-\frac{X^2}{4Dt}\right)} \exp\left(\frac{E_A}{kT}\right) \quad (4)$$

Where L is thickness of oxide, A is area of filament. The retention failure time calculated using Arrhenius behavior from Eq. (4) after some rearrangement is given by:

$$t = \frac{c}{R_{LRS}} \exp\left(\frac{E_A}{kT}\right) \quad (5)$$

Where c depend on geometry of the filament and diffusion coefficient. The diffusion of Cu atoms from the filament decreases the Cu concentration, as a result the LRS current (I_{LRS}) decreases. This can be evaluated by the following equation.

$$I_{LRS} = \frac{V}{L} \int_0^{2\pi} d\theta \int_0^{R_{CF}} \sigma(r) r dr \quad (6)$$

Where V is reading voltage and R_{CF} is radius of filament. Substituting the conductivity expression of Eq. (3) into Eq. (6), I_{LRS} as function of retention time is given by:

$$I_{LRS} = \frac{V}{L} \int_0^{2\pi} d\theta \int_0^{R_{CF}} \gamma \exp\left(\frac{E_A}{kT}\right) \left[\frac{C_0}{\sqrt{\pi Dt}} \exp\left(\frac{-r^2}{4Dt}\right) \right] dr \quad (7)$$

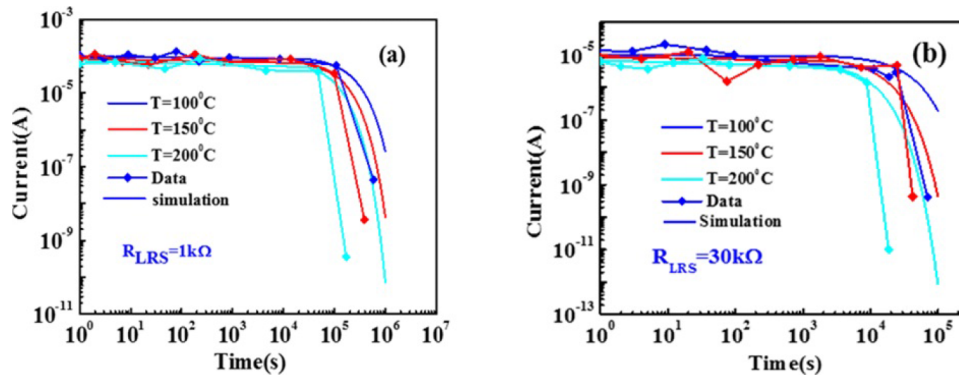


FIG. 4. LRS retention time at different temperature for (a) $R_{LRS}=1k\Omega$ and (b) $R_{LRS}=30k\Omega$.

The degradation of LRS retention behavior corresponding to the decrease of current as function of time is depicted in Fig. 4(a) and 4(b) for various R_{LRS} . As we observe from the figure, the conductance failure accelerates for high R_{LRS} as shown in Fig. 4(b) because of low Cu atoms concentration. According to the model and experimental result, the current of the On-state resistance depends on Cu atom concentration. Thus, retention time improved by making thin filament ($1k\Omega$ resistance) associated with high Cu atoms concentration. For cell with high Cu atoms concentration I_{LRS} was almost constant after 10^4 s, whereas low concentration corresponding to $30k\Omega$, the current starts to decrease before reached 10^4 s, indicating that LRS is degraded.

The importance of Cu concentration in device reliability and the corresponding local temperature of filament was analyzed by COMSOL Multiphysics. Fig. 5(a) shows the calculated conductance as function of retention time during dissolution of filament. The conductance in the figure is gradually changes from point A to B and abruptly drops from B to C, corresponding to the rupture of the filament. Actually the decrease in current occurs due to thermal accelerated out-diffusion of ions. This correction factor allows us to use 2D COMSOL simulations, emulating a 3D filamentary behavior indicated in Fig. 5(b), which correspond to the points A, B and C of Fig. 5(a). Joule heating increases local temperature and the Cu concentration gradient strongly enhances the out-diffusion at the TE/ filament tip interface and disconnects the CF, as shown in Fig. 5(b) C. Filament local temperature increase due to Joule heating is simulated using COMSOL Multiphysics, as shown in Fig. 5(c). For calculation profile of the temperature the top and bottom electrodes act as thermal sinks where the temperature is virtually fixed at room temperature. A, B and C in the Fig. 5(c) indicate local temperature of the filament due to current density corresponding to point A, B and C in Fig. 5(a).

Finally, we analyze the retention time at room temperature (RT) for the On-state resistance according to the power law $R_{ON}=At^n$, where n is slightly greater than zero. The 10-year retention of CBRAM has therefore often been estimated by monitoring the On-state resistance over a relatively short period of time 10^5 s, then extrapolating the power law dependence up to 10 years. Fig. 6 shows the power dependence of On-state resistance at room temperature and experimental result. The acknowledged shortcoming of this approach is that the power law dependence of On-state resistance might not remain valid at very long timescales, making the extrapolation inaccurate. Indeed, instead of increasing steadily with time, the On-state resistance of CBRAM is sometimes observed to fail via an abrupt increase in resistance. Such failures are especially true when a reset bias is applied to the device.¹⁸⁻²¹ This is because of the lowering of the ions migration barrier by external field and thermal energy ion diffusion enhancement through local Joule heating. It is noteworthy that small reading voltage for the read operation is small enough to ignore the influence of the voltage stress on the retention test.

Based on diffusion analysis, we investigate the effect of On-state resistance retention time at different temperature. On-state resistance modulation depends on Cu concentration in the filament. Low Cu concentration shows instability of On-state resistance. This reduction of Cu concentration accelerates at high temperature because of out-diffusion of Cu species from filament enhanced

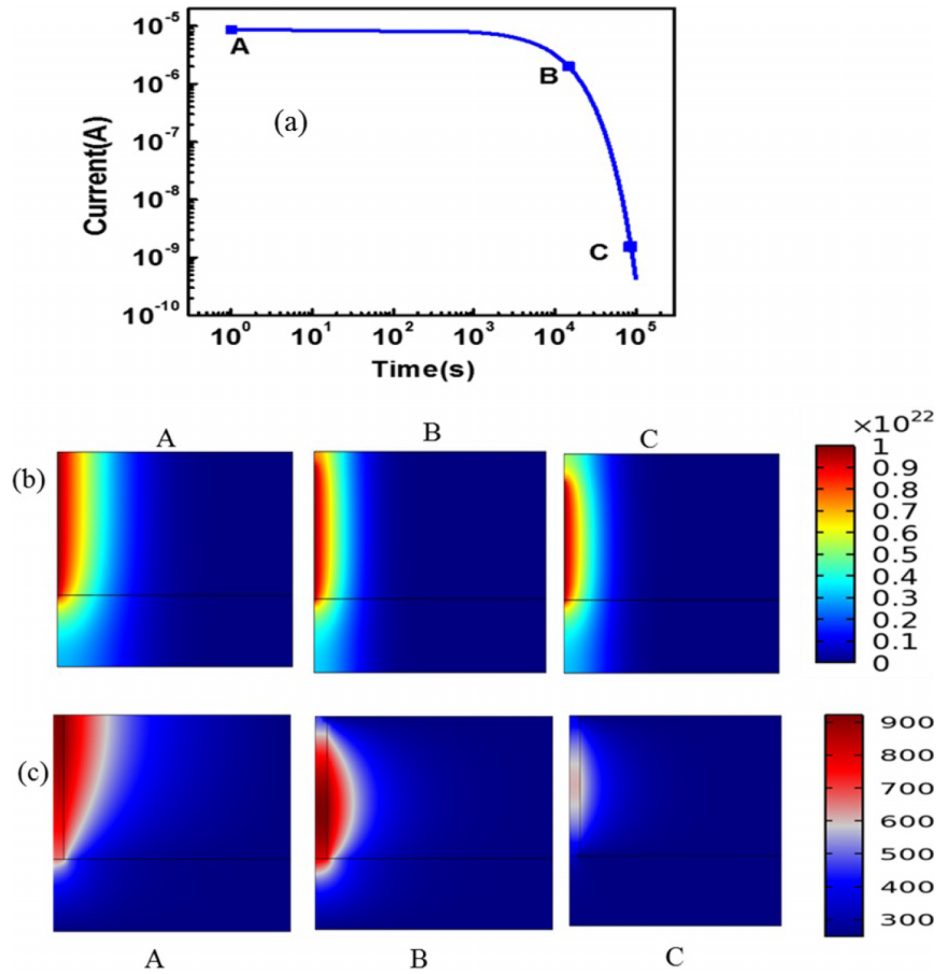


FIG. 5. (a) Calculated device conductance as function of time. (b) Cu defect concentration showing the evolution of the filament at different time using COMSOL Multiphysics. (c) Calculated profile of local temperature of the filament using COMSOL Multiphysics.

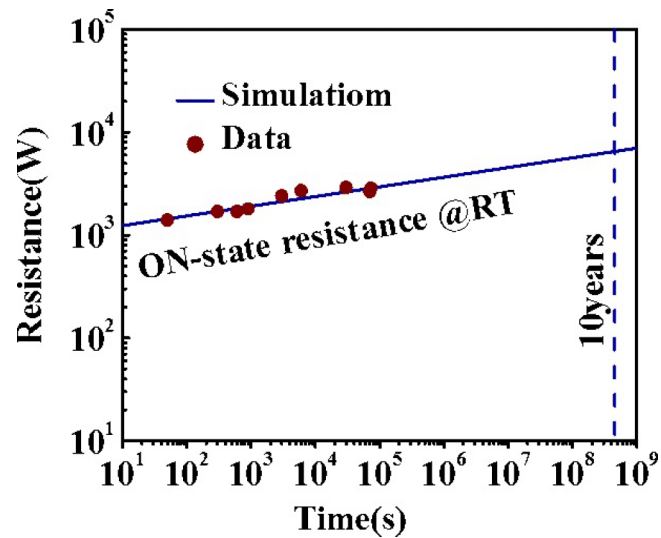


FIG. 6. Data and calculated retention time using power law at room temperature and extrapolation procedure often used to estimate the long term retention.

at high temperature. Modeling the Cu concentration in the filament, we provide a quantitative description of concentration dependent data retention in Cu-based CBRAM. According to our simulation and experimental analysis, better retention time was observed for thin filament and high Cu concentration defect, in which electron wave function associated with Cu⁺ overlap and an extended state formation. This work provides an important step towards enhancing the understanding of the fundamental physics of resistive switching and its future application.

ACKNOWLEDGMENTS

This work was supported by the Future Semiconductor Device Technology Development Program (10045085) funded By MOTIE (Ministry of Trade, Industry & Energy) and KSRC (Korea Semiconductor Research Consortium).

- ¹ M. Kund, G. Beitel, C.-U. Pinnow, T. Röhr, J. Schumann, R. Symanczyk, K.-D. Ufert, and G. Müller, In. IEDM Tech. Dig. 754 (2005).
- ² M. Tada, T. Sakamoto, Y. Tsuji, N. Banno, Y. Saito, Y. Yabe, S. Ishida, M. Terai, S. Kotsuji, N. Iguchi, M. Aono, H. Hada, and N. Kasai, In. IEDM Tech. Dig. 943 (2009).
- ³ Y.-Y. Lin, F.-M. Lee, Y.-C. Chen, W.-C. Chien, C.-W. Yeh, K.-Y. Hsieh, and C.-Y. Lu, In. VLSI Symp. Tech. Dig. 91 (2010).
- ⁴ D. Jana, S. Roy, R. Panja, M. Dutta, S. Z. Rahaman, R. Mahapatra, and S. Maikap, *Nanoscale Res. Lett.* **10**, 188 (2015).
- ⁵ S. Yu and H.-S. Philip Wong, *IEEE Trans. Electron Dev.* **58**, 1352 (2011).
- ⁶ R. Waser and M. Aono, *Nat. Mater.* **6**, 833 (2007).
- ⁷ S. Lim, S. Lee, J. Woo, D. Lee, A. Prakash, and H. Hwang, *ECS Solid state Lett.* **4**, Q25 (2015).
- ⁸ H.-Y. Lee, P.-S. Chen, C.-C. Wang, S. Maikap, P.-J. Tzeng, C.-H. Lin, L.-S. Lee, and M.-J. Tsai, *Jpn. J. Appl. Phys.* **46**, 2175 (2007).
- ⁹ R. Symanczyk, R. Ditrich, J. Keller, M. Kund, G. Müller, B. Ruf, Q. AG, P.-H. Albaredo, S. Bournat, L. Bouteille, and A. Duch, In. Proc. Nonvolatile Memory Technol. Symp. P. 71 (2007).
- ¹⁰ D. Kamalanathan, S. Baliga, S. P. Thermadam, and M. Kozicki, In. Proc. Nonvolatile memory Technol. Symp. 91 (2007).
- ¹¹ D. Ielmini, F. Nardi, C. Cagli, and A. L. Lacaita, *IEEE Electron Dev. Lett.* **31**, 353 (2010).
- ¹² S. Choi, Y. Yang, and W. Lu, *Nanoscale* **6**, 400 (2014).
- ¹³ S. Yu, Y. Y. Chen, X. Guan, H.-S. Philip Wong, and J. A. Kittl, *Appl. Phys. Lett.* **100**, 043507 (2012).
- ¹⁴ Y. Y. Chen, M. Komura, R. Degraeve, B. Govoreanu, L. Goux, A. Fantini, N. Raghavan, S. Clima, L. Zhang, A. Belmonte, A. Redolfi, G. S. Kar, G. Groeseneken, D. J. Wouters, and M. Jurczak, IEDM Tech. Dig. 252 (2013).
- ¹⁵ Z. Wei, T. Ninomiya, S. Muraoka, K. Katayama, R. Yasuhara, and T. Mikawa, IITC/AMC. 349 (2014).
- ¹⁶ B. D. Briggs, S. M. Bishop, K. D. Leedy, and N. C. Cady, *Thin Solid Films* **562**, 519 (2014).
- ¹⁷ S. Larentis, F. Nardi, S. Balatti, D. C. Gilmer, and D. Ielmini, *IEEE Trans. Electron Dev.* **59**, 2468 (2012).
- ¹⁸ X. Xu, H. Lv, H. Liu, T. Gong, G. Wang, M. Zhang, Y. Li, Q. Liu, S. Long, and M. Liu, *IEEE. Electron Dev. Lett.* **36**, 129 (2015).
- ¹⁹ D. Kamalanathan, U. Russo, and D. Ielmini, *IEEE Electron Dev. Lett.* **30**, 553 (2009).
- ²⁰ N. Banno, T. Sakamoto, S. Fujieda, and M. Aono, Annual Int. Reliability physics Symp. 707 (2008).
- ²¹ Y. Koo, S. Ambrogio, J. Woo, J. song, D. Ielmini, and H. Hwang, *IEEE Electron Dev. Lett.* **36**, 238 (2015).